2021 43rd Annual International Conference of the
IEEE Engineering in Medicine & Biology Society (EMBC)
Oct 31 - Nov 4, 2021. Virtual Conference

2021 43rd Annual International Conference of the IEEE Engineering in Medicine & Biology Society (EMBC) | 978-1-7281-1179-7/21/$31.00 ©2021 IEEE | DOI: 10.1109/EMBC46164.2021.9630982

Basic study of epileptic seizure detection using a single-channel frontal EEG and a pre-trained ResNet*

Takumu Yoshiba, Hiroaki Kawamoto, and Yoshiyuki Sankai, *Member, IEEE*

***Abstract*— Epilepsy is a neurological disorder that causes sudden seizures due to abnormal excitation of neurons in the brain. Approximately 30 % of patients cannot control their seizures using medication. In addition, since seizures can occur anywhere and at any time, caregivers must always be with the patient. Various researchers have developed seizure detection methods using multichannel EEG to improve the quality of life of patients and caregivers. However, the large size of the measurement device impedes transportation. We believe that a portable measurement device with a small number of channels is suitable for detecting seizures in daily life. Therefore, we need a system that can detect seizures using a small number of channels. The purpose of this research is to develop a seizure detection algorithm using a single-channel frontal EEG and to confirm its basic performance. We used EEG signals from a single electrode position (Fp1-F7, Fp2-F8), which is a bipolar derivation of the frontal region. We segmented the EEG using a 2 s sliding window with 50 % overlap and converted the segments into images. After preprocessing, we fine-tuned ResNet18, pre-trained on ImageNet, and developed an ensemble classification method. In the experiments with 10 epileptic patients (3 – 19 years old) registered in the CHB-MIT scalp EEG database, the results showed that the average sensitivity was 88.73 %, the average specificity was 98.98 %, and the average detection latency time was 7.39 s. In conclusion, the developed algorithm was validated as sufficiently accurate to detect epileptic seizures.**

***Clinical Relevance*— This establishes an image recognition algorithm that can detect epileptic seizures using a single-channel frontal EEG.**

I. Introduction

Epilepsy is a neurological disorder that causes sudden seizures due to the abnormal excitation of neurons in the brain. According to the World Health Organization, approximately 50 million people are estimated to have epilepsy worldwide [1]. Seizure symptoms vary widely, including tonic-clonic, absence, myoclonic, and atonic seizures. Many patients can live a seizure-free life if properly diagnosed and treated; however, approximately 30 % of patients cannot control their seizures with medication; this is an obstacle to their social lives. In addition, after a seizure, caregivers need to ensure the patient's safety as the patients are at risk of bumping into objects or drowning in the bath, for example. However, since seizures can occur anywhere and at any time, caregivers must always be with the patient, which limits their daily activities. Therefore, seizure detection systems are needed to improve the quality of life of patients and caregivers. Various researchers have developed seizure detection methods using multichannel EEG [2–3]. These methods can detect seizures with greater accuracy than single-channel EEGs as multichannel EEGs contain more signal information. However, the measurement device is quite large, and the electrodes must be placed on the entire head. In addition, since EEG measurement is usually performed in a hospital, the measurement location is limited. Therefore, it is difficult to measure EEG signals during daily life. We believe that a portable measurement device with a small number of channels is suitable for detecting seizures in daily life. Thus, we require a system that can detect seizures using a small number of channels.

To solve this problem, we focused on frontal EEGs. The frontal association cortex is a region of the brain that receives information from other association cortexes and makes action plans based on the input [4–5]. It is also interconnected with the motor cortex, basal ganglia, and limbic system through fiber connections and receives information regarding movement, memory, arousal, and adjusting autonomic nerves [6]. Therefore, we consider that abnormal nerve excitation propagates to the frontal association area when uncontrolled jerking movements and loss of consciousness — i.e., seizure symptoms — occur. In addition, since the frontal association cortex is interconnected with other regions of the brain, we consider that abnormal nerve excitation sometimes propagates to the frontal association cortex when focal seizures occur in another region. Therefore, we believe that epileptic seizures can be detected using frontal EEG. It is easier to place electrodes on the forehead than on other measurement points because the skin is exposed. Therefore, frontal EEG seems to be the most appropriate method for seizure detection during daily life.

In previous studies, statistical or frequency domain features extracted from multichannel EEGs have been used to detect seizures [3]. In addition, various supervised and unsupervised learning methods such as support vector machines, random forests, and k-nearest neighbor algorithms have been used as classifiers to detect seizures with high accuracy. However, since the information obtained from single-channel EEGs is less than that of multichannel EEGs, it is necessary to extract features more efficiently. In current EEG examinations, clinical investigators who have both experience and clinical knowledge diagnose seizure types based on EEG findings. Abnormal epileptic EEGs have a

* A part of this research was funded by ImPACT Program, promoted by Council for Science, Technology and Innovation, Cabinet Office, Japan.

T. Yoshiba is Second years in the Master of Graduate School of Systems and Information Engineering, University of Tsukuba, 1-1-1 Tennodai, Tsukuba, 305-8577, Japan. (e-mail: yoshiba@golem.iit.tsukuba.ac.jp).

H. Kawamoto is with Faculty of Engineering, Information and Systems and Center for Cybernics Research, University of Tsukuba, 1-1-1 Tennodai, Tsukuba, 305-8577, Japan (e-mail: kawamoto@golem.iit.tsukuba.ac.jp).

Y. Sankai is with Faculty of Engineering, Information and Systems and Center for Cybernics Research, University of Tsukuba, 1-1-1 Tennodai, Tsukuba, 305-8577, Japan. (e-mail: sankai@golem.iit.tsukuba.ac.jp).

complex wave patterns that comprise combination of spikes and slow waves [7], which are easy to distinguish from the background activity of normal EEG. Therefore, we believed that pattern recognition method is one of the most suitable for seizure detection. In recent years, advances in computing power have led to the development of deep learning methods for automatic pattern recognition. It has been confirmed that the performance of image recognition techniques is high enough to surpass that of humans [8–9]. Therefore, we believe that an image recognition technique that automatically learns abnormal wave patterns from EEG images is suitable for seizure detection using single-channel EEGs.

The purpose of this research was to develop an image recognition algorithm for detecting epileptic seizures using a single-channel frontal EEG and to confirm its basic performance.

II. Materials and Methods

A. EEG data

In this study, we used the CHB-MIT Scalp EEG database from PhysioNet.org [10]. In this database, EEG data were measured from pediatric patients with intractable seizures based on the international 10 – 20 system [11]. They were recorded with a sampling frequency of 256 Hz and a resolution of 16 bits. The EEG data were stored in European Data Format (EDF) files, and the power line noise in EEG data was already removed. We used EEG signals from a single electrode position (Fp1-F7, Fp2-F8), which is a bipolar derivation of the frontal region. The position of the channel is shown in Fig. 1.

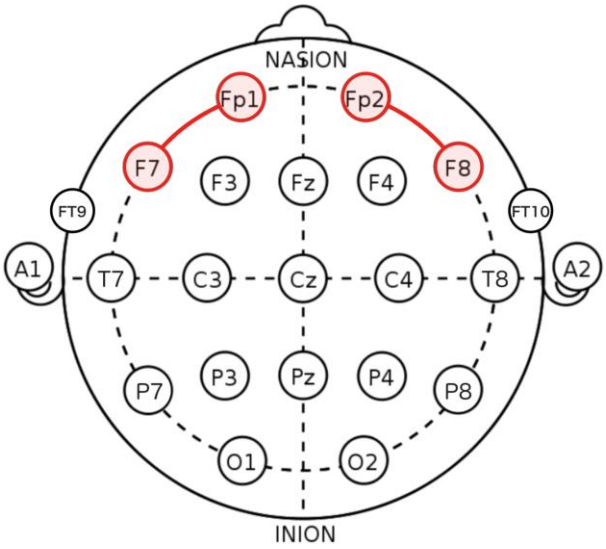

Figure 1. The position of Fp1-F7 and Fp2-F8

There are two phases in epilepsy: the ictal period (during a seizure) and the interictal period (between seizures). The ictal period is the period between the onset of the first symptom and the end of the seizure. During the ictal period, abnormal epileptic EEGs appear in some or all of the brain. Since the database contains annotation files regarding the start and end times of seizures, as identified by clinical investigators, we used this information to identify the ictal period. The interictal period is defined as the period between the end of the seizure and the onset of the next seizure. It accounts for 99 % of the patients' daily lives. Before the onset of a seizure, some patients experience physical, sensory, or emotional changes. Therefore, the period immediately before the seizure should be excluded from the interictal period. In addition, since the patient is dazed and gradually regains consciousness after the seizure [12], it takes time to return to normal brain activity. For these reasons, we defined the interictal period as a period of more than 30 min from the beginning and end of the seizure (Fig. 2).

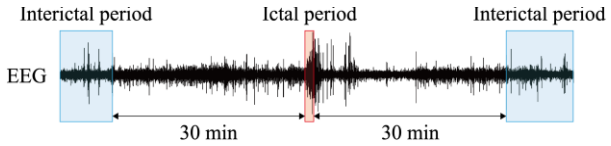

Figure 2. Ictal and Interictal period

B. Epileptic abnormal waves

We focused on the shape of the abnormal EEG that appeared during the ictal period. Neurons become overexcited due to repetitive paroxysmal depolarizing shifts in the epileptic focus, resulting in epileptic discharges, such as spikes and sharp waves [7]. In addition, slow waves occur during hyperpolarization. Since an epileptic abnormal EEG comprises this combination of spikes and slow waves, it can be clearly distinguished from the background activity of a normal EEG. The types of abnormal EEGs that appear during generalized seizures are shown in Table I [13–14]. The spike-and-slow-wave complex (sp-w) occurs during a generalized tonic-clonic seizure and 3 Hz sp-w occurs during an absence seizure. Polyspike EEG patterns are commonly observed in juvenile myoclonic epilepsy. In addition, the delta and theta bursts are high-amplitude, rhythmic slow waves that occur when brain function is impaired, such as loss of consciousness. Characteristic abnormal EEG patterns occur during each type of seizure and thus we developed an image recognition algorithm to classify the shape of normal and epileptic abnormal EEGs.

TABLE I.
Types of Epileptic Abnormal EEGs

Name	sp-w	3Hz sp-w	polyspike	δ burst	θ burst
Waveform					

C. Signal processing

We segmented the EEG using a 2-second sliding window with a 50 % overlap. An overview of the EEG segmentation is shown in Fig. 3. The amplitude of normal scalp EEG is about 10 to 100 μV and abnormal EEG often has an amplitude more than twice as large as the background activity of a normal EEG. Therefore, we imaged the segmented EEG in the range of ±600 μV to have enough area to display the EEG. During imaging, the background color was set to black and the EEG was set to white. In addition, we resized the EEG image to 256 × 256 and cropped the center to 244 × 244. We used a pre-trained model from the Pytorch torchvision library and thus used the mean and standard deviation of the training data RGB levels from ImageNet to normalize the input images [15].

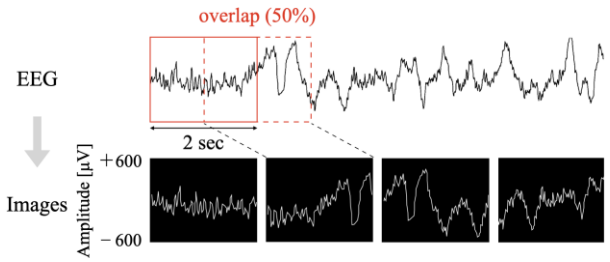

Figure 3. An overview of EEG segmentation

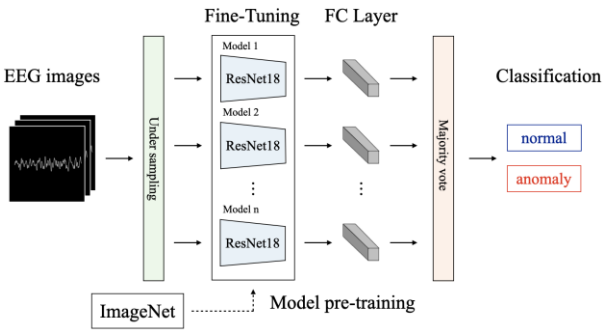

Figure 4. Model architecture

D. Development of the classifier

The model architecture is illustrated in Fig. 4. Since the interictal period accounts for most of the patients' daily lives, the amount of ictal EEG data that can be collected from patients is very small and the dataset has an imbalanced proportion of data. If an imbalanced dataset is used for training a classifier, the classification accuracy will be low. Therefore, it is necessary to balance the data proportion [16]. To prevent overfitting, and use all available EEG data, we undersampled the interictal EEG data to match the number of ictal EEG data, created *n* sub-datasets, trained each classifier using each sub-dataset, and then determined the final output by taking a majority vote on the output of all classifiers.

The amount of data in each sub-dataset was small so the batch size was set to 8. In addition, to detect abnormal epileptic EEGs using image recognition techniques, we used ResNet18 as a classifier. ResNet (Residual Network) is a neural network model devised by Kaiming He et al. in 2015 [8], which achieves deeper layers and improved accuracy by introducing a shortcut connection. There are five versions of pre-trained models available in the Pytorch Torchvision library: 18, 34, 50, 101, and 152 layers. As the layers get deeper, it takes more time to train the model; we decided to use ResNet with 18 layers as a classifier. We loaded the pre-trained ImageNet weights from the torchvision model subpackage. ResNet is a model created for classifying an input image into 1,000 categories so we need to replace the output layer for two-class classification. Therefore, we created a linear layer with two output nodes and replaced it with the output layer of ResNet18.

During training, our model calculated the loss per epoch and performed backpropagation. During validation, our model calculated the accuracy per epoch using validation data and saved the weight parameter of the model when the accuracy improved. The number of epochs was set to 50. Seizure detection is a binary classification task so we used cross-entropy loss as the loss function. In addition, we used ADAM as the optimizer to minimize the loss function and set the learning rate to 0.005. In this study, we fine-tuned ResNet trained on the ImageNet dataset for each patient to create a classifier tailored to the patient's seizure symptoms.

E. Seizure detection algorithm

The EEG contains superimposed noise due to head movement, facial muscle tension, and blinking [17] and thus evaluation within a single window is insufficient to classify normal and abnormal EEGs. Therefore, we developed a seizure detection algorithm to expand the decision range (Fig. 5). In Fig. 5, we define the classes estimated by the ensemble model as class 0 (normal) and class 1 (anomaly). The proposed algorithm comprises two phases. The role of Phase I is to judge the timing of the change from the interictal period to the ictal period and the role of Phase II is to judge the timing of the change from the ictal period to the interictal period.

I) When class 1 is counted five times in a row, our algorithm determines an anomalous EEG and moves to phase II. Otherwise, our algorithm determines a normal EEG signal.

II) When class 0 is counted *N* times in a row, our algorithm determines a normal EEG and moves to phase I. Otherwise, our algorithm determines an anomalous EEG. *N* is the number of times class 1 is counted after moving to phase II.

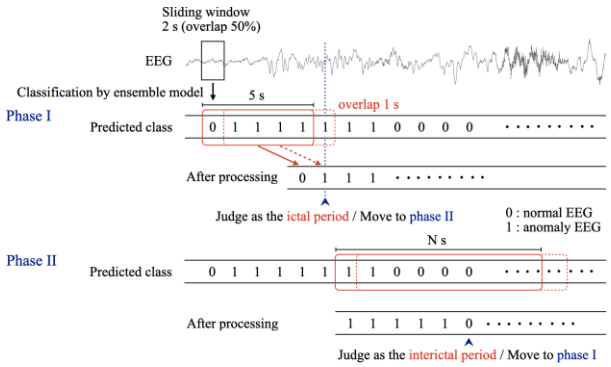

Figure 5. Seizure detection algorithm

F. Experiment

To confirm whether the developed algorithm is sufficiently accurate to detect abnormal EEG, we conducted experiments with 10 epileptic patients (3 – 19 years old) registered in the CHB-MIT scalp EEG database. The patient information is presented in Table II. We conducted two experiments, one using the Fp1-F7 channel and the other using the Fp2-F8 channel. To evaluate the developed algorithm, we performed leave-one-out cross-validation (LOOCV). The procedure is as follows: First, we created *N* subgroups, where *N* is the number of seizures in each patient. Next, we divided the *N* seizure data into subgroups. We then divided the non-seizure data into subgroups so that the total time of non-seizure data in each group was equal. For example, in the case of chb01, the dataset contains seven edf files containing the ictal EEG (chb01_03.edf, chb01_04.edf, chb01_15.edf, chb01_16.edf, chb01_18.edf, chb01_21.edf, chb01_26.edf), we created seven subgroups and divided the seizure data into subgroups. In addition, since the dataset contains 21 hours of non-seizure

data, we divided the 21 h of EEG data into 3 h of EEG data for each subgroup. We used one of the *N* subgroups as validation data and the others as training data. This cross-validation process was repeated *N* times, with each of the *N* subgroups used once as validation data. We evaluated sensitivity, specificity, and detection latency time (DLT). The sensitivity, specificity, and DLT were defined as follows:

$$Sensitivity = \frac{TP}{TP + FN} \times 100 \quad (1)$$

$$Specificity = \frac{TN}{TN + FP} \times 100 \quad (2)$$

$$DLT = |T_s - T_d| \quad (3)$$

where *TP* is the number of true positives, *FP* is the number of false positives, *TN* is the number of true negatives, and *FN* is the number of false negatives. In addition, T_s is the time of seizure onset and T_d is the time when the seizure is first detected.

TABLE II.
PATIENT'S INFORMATION

ID	*Gender*	*Age*	*Number of seizures*	*Average time of ictal EEG [s]*	*Total time of interictal EEG [h]*
chb01	F	11	7	63.14	21
chb02	M	11	2	81.50	18
chb03	F	14	7	57.43	21
chb05	F	7	5	111.60	20
chb07	F	14	3	108.33	48
chb08	M	3	5	120.00	10
chb09	F	10	4	69.00	32
chb13	F	3	10	33.54	20
chb19	F	19	3	78.67	18
chb22	F	9	3	68.00	18

G. EEG reading

To determine the seizure type of epilepsy, it is necessary to estimate epileptic foci via electroencephalography. In this study, 18 channel EEGs were read for each patient to estimate their epileptic foci. EEG readings were performed based on the following criteria: the phase reversal between channels, large amplitude (>200 μV), appearance of spiny waves, sharp waves, and other abnormal epileptic EEGs [18]. As an example, the ictal period EEG of chb01 is shown in Fig. 6. The seizure started at 2996 s and a phase reversal of high-amplitude EEG (±200 μV) was identified between Fp2-F4 and F4-C4 immediately after onset. Five seconds after the onset of the seizure, polyspikes appeared at Fp2-F8 and F8-T8. For these reasons, we suggest that the epileptic foci were in the vicinity of F4 and F8. The ictal period EEG of chb05 is shown in Fig. 7. The seizure started at 2317 s and polyspikes appeared between F7-T7 and T7-P7 and between F8-T8 and T8-P8 immediately after the onset. In addition, spikes and slow-wave complexes were identified over the entire head 4 s after the onset of the seizure. For these reasons, we suggest that the seizure foci were located in T7 and T8. Thus, we performed EEG readings for all 10 patients.

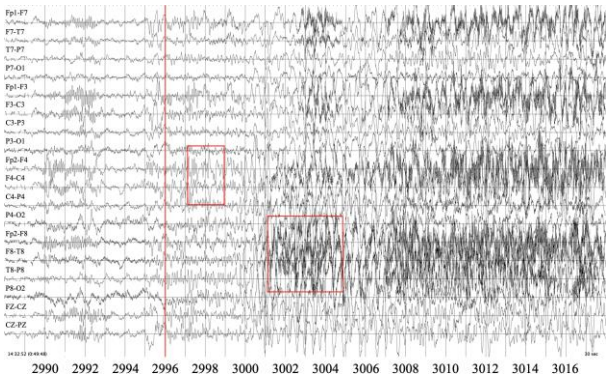

Figure 6. The ictal period EEG of chb01

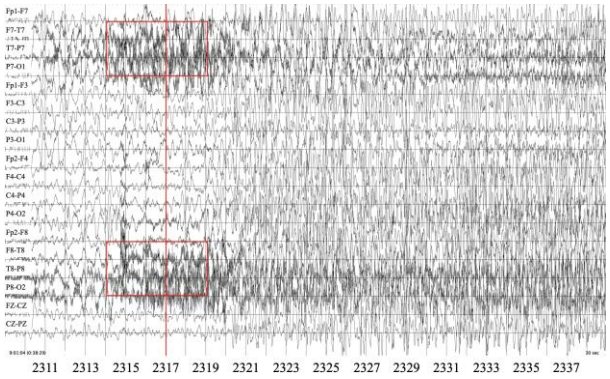

Figure 7. The ictal period EEG of chb05

III. RESULTS

The results of the experiment using the Fp1-F7 channel are presented in Table III. The average sensitivity was 88.08 %, the average specificity was 98.98 %, and the average DLT was 7.55 s. The results of the experiment using the Fp2-F8 channel are presented in Table IV. The average sensitivity was 86.63 %, the average specificity was 97.76 %, and the average DLT was 8.16 seconds. The results of selecting the better channel in terms of sensitivity and specificity for each patient are presented in Table V. The average sensitivity, specificity, and DLT were 88.73 %, 98.98 %, and 7.39 s, respectively. The results of the EEG reading for 10 patients are presented in Table VI. F7, T7, and P7 indicate the anterior, middle, and posterior temporal regions of the left hemisphere, respectively, and F8, T8, and P8 indicate the anterior, middle, and posterior temporal regions of the right hemisphere. From the results of the EEG readings, it was estimated that all 10 patients had epileptic foci in the temporal region.

TABLE III.
RESULTS OF EXPERIMENT USING FP1-F7

ID	*Sensitivity [%]*		*Specificity [%]*		*DLT [s]*	
	Average	*S.D.*	*Average*	*S.D.*	*Average*	*S.D.*
chb01	89.67	5.63	98.55	2.71	6.29	1.50
chb02	86.33	0.12	99.06	0.85	12.00	0.00
chb03	90.29	4.39	98.86	2.14	5.43	1.13
chb05	90.18	4.69	99.11	1.28	9.80	4.44
chb07	90.37	8.28	99.38	0.43	6.33	0.58
chb08	94.62	2.11	98.22	1.81	7.40	2.51
chb09	87.63	7.53	99.61	0.73	9.00	4.24
chb13	82.21	6.81	99.26	0.74	6.10	0.57
chb19	86.24	3.84	98.85	1.07	9.67	0.58
chb22	85.65	6.84	99.15	0.83	11.00	5.57
ALL	88.08	6.36	98.98	1.51	7.55	3.01

TABLE IV.
RESULTS OF EXPERIMENT USING FP2-F8

ID	*Sensitivity [%]*		*Specificity [%]*		*DLT [s]*	
	Average	*S.D.*	*Average*	*S.D.*	*Average*	*S.D.*
chb01	90.80	5.63	95.64	10.17	5.43	1.13
chb02	87.58	1.65	98.20	0.44	11.00	1.41
chb03	88.08	6.26	97.67	2.73	7.57	3.26
chb05	90.09	5.60	94.78	9.43	9.00	4.74
chb07	94.13	4.14	99.56	0.41	6.67	2.89
chb08	92.27	1.82	97.22	2.80	10.20	2.17
chb09	90.57	6.42	99.60	0.70	7.00	4.00
chb13	73.78	15.77	99.30	0.95	8.70	1.95
chb19	89.27	1.45	98.78	1.55	9.33	1.15
chb22	85.18	7.00	97.99	1.09	9.33	4.04
ALL	86.63	10.54	97.76	4.99	8.16	3.01

TABLE V.
RESULTS OF SELECTED CHANNELS

ID	*Sensitivity [%]*		*Specificity [%]*		*DLT [s]*		*side*
	Average	*S.D.*	*Average*	*S.D.*	*Average*	*S.D.*	
chb01	89.67	5.63	98.55	2.71	6.29	1.50	left
chb02	86.33	0.12	99.06	0.85	12.00	0.00	left
chb03	90.29	4.39	98.86	2.14	5.43	1.13	left
chb05	90.18	4.69	99.11	1.28	9.80	4.44	left
chb07	94.13	4.14	99.56	0.41	6.67	2.89	right
chb08	94.62	2.11	98.23	1.81	7.40	2.51	left
chb09	90.57	6.42	99.60	0.70	7.00	4.00	right
chb13	82.21	6.81	99.26	0.74	6.10	0.57	left
chb19	89.27	1.45	98.78	1.55	9.33	1.15	right
chb22	85.65	6.84	99.15	0.83	11.00	5.57	left
ALL	88.73	6.22	98.98	1.53	7.39	3.01	

TABLE VI.
ESTIMATED SEIZURE FOCI

ID	*Estimated seizure foci*
chb01	F4, F8
chb02	P3, P7
chb03	P7
chb05	T7, T8
chb07	T7, T8
chb08	T7
chb09	T7, T8
chb13	F7
chb19	F7, F8
chb22	T7, T8

IV. DISSCUSION

To detect seizures, several methods using multichannel EEG have been developed. Zabihi et al. developed a method to extract statistical and frequency domain features from EEG and created a classifier for each patient using SVM [3]. They conducted experiments with four epileptic patients registered in the CHB-MIT scalp EEG database. The average sensitivity and specificity were 90.62 % and 99.32 %, respectively. These methods using multi-channel EEG can be applied to the automatic interpretation of EEG and the diagnosis of epilepsy. However, it is difficult to measure multichannel EEG during daily life because the measurement device is quite large and electrodes must be placed on the entire head. For these reasons, we proposed an algorithm to detect seizures using a single-channel frontal EEG. As a result of the experiment, the average sensitivity of developed algorithm was 88.73 %, which confirmed that the developed algorithm was as sensitive as the conventional method using multichannel EEG. Since abnormal epileptic EEGs can be clearly distinguished from the background activity of a normal EEG, we believe that we were able to achieve highly sensitive seizure detection based on the waveform pattern. In addition, we confirmed that the DLT of developed algorithm was 7.39 s. Since epileptic seizures usually last from 30 to 60 s, if we can notify a caregiver within 8 s after onset, the caregiver can quickly take care of the patient after the seizure. Therefore, we consider that the time delay of our algorithm is not a problem for seizure detection. We believe that our proposed method using single-channel frontal EEG will contribute to the detection of epileptic seizures during daily life. Meanwhile, the experimental results show that the average specificity of developed algorithm was 98.98 %, which was lower than that of conventional methods. One reason for this is that there is little brain activity information available from a single-channel EEG and another reason is that the EEG contains superimposed noise due to head movement, facial muscle tension, and blinking [16]. To improve the specificity, we believe that it is necessary to increase the width of the sliding window used in the seizure detection algorithm.

In this study, we examined EEG signals to estimate the location of epileptic foci in patients. As a result of the EEG reading, all 10 patients were estimated to have epileptic foci in the temporal region. Therefore, we believe that the algorithm developed using a single-channel frontal EEG can detect

temporal lobe seizures. There are two types of temporal lobe epilepsy: mesial temporal lobe epilepsy, in which seizures are triggered by hippocampal stiffness in the limbic system [19], and lateral temporal lobe epilepsy, in which seizures are caused by epileptic discharges in the neocortex. Since the frontal association cortex is interconnected with the temporal association cortex and limbic system by fiber connections, we believe that abnormal excitations propagate to the frontal association cortex when epileptic discharges occur in the temporal region. In the case of detecting temporal lobe seizures, some studies have shown that using a single-channel temporal EEG (FT10-T8) is effective [20]; however, when measuring the temporal channel, it is not easy to place electrodes on the measurement points because of the patient's hair. Therefore, compared to the methods using other single-channel EEG, our algorithm using single-channel frontal EEG is effective for detecting temporal lobe seizures during daily life in terms of ease of placement.

The basic performance of the developed algorithm was experimentally confirmed. In the future, we will collect frontal EEG data of patients with epilepsy during their daily lives and verify the accuracy of the proposed algorithm.

V. Conclusion

We proposed and developed an algorithm to detect abnormal epileptic EEG patterns using single-channel frontal EEG and image recognition techniques. The experimental results showed that our algorithm was as sensitive as the conventional method using multi-channel EEG. In addition, we estimated the location of the epileptic foci via EEG reading and demonstrated the possibility of detecting temporal lobe epilepsy. In the future, we will collect frontal EEG data of epileptic patients during their daily lives and verify the accuracy of the proposed algorithm.

Appendix

Details of the experimental subgroups are presented in Table VII. Each subgroup contained different seizure data. Because some edf files contain two or more seizures, some of the names in the Seizure data columns are the same.

TABLE VII.
ESTIMATED SEIZURE FOCI

ID	*Subgroup number*	*Seizure data*	*Non seizure data*
chb01	1	chb01_03.edf	chb01_06.edf, chb01_07.edf, chb01_08.edf
	2	chb01_04.edf	chb01_09.edf, chb01_10.edf, chb01_11.edf
	3	chb01_15.edf	chb01_12.edf, chb01_13.edf, chb01_23.edf
	4	chb01_16.edf	chb01_24.edf, chb01_30.edf, chb01_31.edf
	5	chb01_18.edf	chb01_32.edf, chb01_33.edf, chb01_34.edf
	6	chb01_21.edf	chb01_36.edf, chb01_37.edf, chb01_38.edf
	7	chb01_26.edf	chb01_39.edf, chb01_40.edf, chb01_41.edf
chb02	1	chb02_16.edf	chb02_02.edf, chb02_07.edf, chb02_08.edf, chb02_09.edf, chb02_10.edf, chb02_11.edf, chb02_12.edf, chb02_13.edf, chb02_14.edf
	2	chb02_16+.edf	chb02_22.edf, chb02_25.edf, chb02_28.edf, chb02_29.edf, chb02_30.edf, chb02_31.edf, chb02_32.edf, chb02_33.edf, chb02_34.edf
chb03	1	chb03_01.edf	chb03_06.edf, chb03_07.edf, chb03_08.edf
	2	chb03_02.edf	chb03_09.edf, chb03_10.edf, chb03_11.edf
	3	chb03_03.edf	chb03_12.edf, chb03_13.edf, chb03_14.edf
	4	chb03_04.edf	chb03_15.edf, chb03_16.edf, chb03_17.edf
	5	chb03_34.edf	chb03_18.edf, chb03_19.edf, chb03_20.edf
	6	chb03_35.edf	chb03_22.edf, chb03_23.edf, chb03_24.edf
	7	chb03_36.edf	chb03_29.edf, chb03_30.edf, chb03_31.edf
chb05	1	chb05_06.edf	chb05_08.edf, chb05_09.edf, chb05_10.edf, chb05_11.edf
	2	chb05_13.edf	chb05_20.edf, chb05_24.edf, chb05_25.edf, chb05_26.edf
	3	chb05_16.edf	chb05_27.edf, chb05_28.edf, chb05_29.edf, chb05_30.edf
	4	chb05_17.edf	chb05_31.edf, chb05_32.edf, chb05_33.edf, chb05_34.edf
	5	chb05_22.edf	chb05_35.edf, chb05_36.edf, chb05_37.edf, chb05_38.edf
chb07	1	chb07_12.edf	chb07_01.edf, chb07_02.edf, chb07_03.edf, chb07_04.edf
	2	chb07_13.edf	chb07_06.edf, chb07_07.edf, chb07_08.edf, chb07_09.edf
	3	chb07_19.edf	chb07_10.edf, chb07_15.edf, chb07_16.edf, chb07_17.edf
chb08	1	chb08_02.edf	chb08_04.edf, chb08_10.edf
	2	chb08_05.edf	chb08_15.edf, chb08_16.edf
	3	chb08_11.edf	chb08_17.edf, chb08_18.edf
	4	chb08_13.edf	chb08_19.edf, chb08_20.edf
	5	chb08_21.edf	chb08_23.edf, chb08_24.edf
chb09	1	chb09_06.edf	chb09_03.edf, chb09_04.edf
	2	chb09_08.edf	chb09_09.edf, chb09_10.edf
	3	chb09_08.edf	chb09_13.edf, chb09_14.edf
	4	chb09_19.edf	chb09_16.edf, chb09_17.edf
chb13	1	chb13_19.edf	chb13_03.edf, chb13_04.edf
	2	chb13_21.edf	chb13_05.edf, chb13_06.edf
	3	chb13_40.edf	chb13_07.edf, chb13_08.edf
	4	chb13_40.edf	chb13_09.edf, chb13_10.edf
	5	chb13_55.edf	chb13_11.edf, chb13_12.edf
	6	chb13_55.edf	chb13_13.edf, chb13_14.edf
	7	chb13_59.edf	chb13_15.edf, chb13_16.edf
	8	chb13_60.edf	chb13_24.edf, chb13_30.edf
	9	chb13_62.edf	chb13_36.edf, chb13_37.edf
	10	chb13_62.edf	chb13_38.edf, chb13_47.edf
chb19	1	chb19_28.edf	chb19_06.edf, chb19_07.edf, chb19_08.edf, chb19_09.edf, chb19_10.edf, chb19_11.edf
	2	chb19_29.edf	chb19_12.edf, chb19_13.edf, chb19_14.edf, chb19_15.edf, chb19_16.edf, chb19_17.edf
	3	chb19_30.edf	chb19_21.edf, chb19_22.edf, chb19_23.edf, chb19_24.edf, chb19_25.edf, chb19_26.edf
chb22	1	chb22_20.edf	chb22_02.edf, chb22_03.edf, chb22_04.edf, chb22_05.edf, chb22_06.edf, chb22_07.edf
	2	chb22_25.edf	chb22_08.edf, chb22_09.edf, chb22_10.edf, chb22_16.edf, chb22_17.edf, chb22_18.edf
	3	chb22_38.edf	chb22_22.edf, chb22_23.edf, chb22_27.edf, chb22_28.edf, chb22_29.edf, chb22_30.edf

REFERENCES

[1] Epilepsy - World Health Organization, https://www.who.int/news-room/fact-sheets/detail/epilepsy

[2] Zabihi M, Kiranyaz S, Ince T, Gabbouj M (2013) Patient-specific epileptic seizure detection in long-term eeg recording in paediatric patients with intractable seizures.

[3] M. K. Siddiqui, R. Morales-Menendez, X. Huang and N. Hussain. (2020, May). "A review of epileptic seizure detection using machine learning classifiers," Brain Inform. [Online]. 7(1), p. 5. Available: https://www.ncbi.nlm.nih.gov/pmc/articles/PMC7248143/. doi: 10.1186/s40708-020-00105-1.

[4] C. F. Jacobsen, "Functions of frontal association area in primates," Arch Neurol Psychiatry, vol. 33, no. 3, pp. 558–569, 1935, doi:10.1001/archneurpsyc.1935.02250150108009.

[5] M. Takada, [Neuroanatomy of Frontal Association Cortex], Brain Nerve, vol. 68, no. 11, pp. 1253－1261, Nov. 2016. Japanese. doi: 10.11477/mf.1416200588. PMID: 27852016.

[6] S. V. Siddiqui et al. "Neuropsychology of prefrontal cortex," Indian J Psychiatry. 2008 Jul;50(3):202-8. doi: 10.4103/0019-5545.43634. PMID: 19742233; PMCID: PMC2738354.

[7] H. Kubista, S. Boehm and M. Hotka. (2019, Jan.). "The Paroxysmal Depolarization Shift: Reconsidering Its Role in Epilepsy, Epileptogenesis and Beyond," Int J Mol Sci. [Online]. 20(3), p. 577. Available: https://www.ncbi.nlm.nih.gov/pmc/articles/PMC6387313/. doi: 10.3390/ijms20030577.

[8] K. He, X. Zhang, S. Ren and J. Sun, "Deep Residual Learning for Image Recognition," 2016 IEEE Conference on Computer Vision and Pattern Recognition (CVPR), Las Vegas, NV, 2016, pp. 770-778, doi: 10.1109/CVPR.2016.90.

[9] What I learned from competing against a ConvNet on ImageNet, http://karpathy.github.io/2014/09/02/what-i-learned-from-competing-against-a-convnet-on-imagenet.

[10] A. Shoeb and J. Guttag, "Application of Machine Learning to Epileptic Seizure Onset Detection," 27th International Conference on Machine Learning (ICML), June 21-24, 2010, Haifa, Israel.

[11] G. Klem et al. "The ten-twenty electrode system of the International Federation. The International Federation of Clinical Neurophysiology," Electroencephalogr Clin Neurophysiol Suppl 52, pp. 3-6, 1999.

[12] Pottkämper JCM, Hofmeijer J, van Waarde JA, van Putten MJAM. The postictal state - What do we know? Epilepsia. 2020 Jun;61(6):1045-1061. doi: 10.1111/epi.16519. Epub 2020 May 12. PMID: 32396219; PMCID: PMC7317965.

[13] J. W. Britton, L. C. Frey, J. L. Hopp et al. (authors); E. K. St. Louis, L. C. Frey (editors) (2016). Electroencephalography (EEG): An Introductory Text and Atlas of Normal and Abnormal Findings in Adults, Children, and Infants [Online]. Chicago: American Epilepsy Society. Available: https://www.ncbi.nlm.nih.gov/books/NBK390347/.

[14] P. D. Emmady and A. C. Anilkumar. "EEG Abnormal Waveforms," in StatPearls [Online]. Treasure Island (FL): StatPearls Publishing, 2020. Available: https://www.ncbi.nlm.nih.gov/books/NBK557655/.

[15] ResNet | PyTorch, https://pytorch.org/hub/pytorch_vision_resnet/

[16] S. Wang, K. Tang and X. Yao, "Diversity exploration and negative correlation learning on imbalanced data sets," in IJCNN'09, pp. 1796－1803.

[17] Kaya, Ibrahim. (2019). A Brief Summary of EEG Artifact Handling. 10.13140/RG.2.2.25108.04484.

[18] Tatum WO, Olga S, Ochoa JG, Munger Clary H, Cheek J, Drislane F, Tsuchida TN. American Clinical Neurophysiology Society Guideline 7: Guidelines for EEG Reporting. J Clin Neurophysiol. 2016 Aug;33(4):328-32. doi: 10.1097/WNP.0000000000000319. PMID: 27482790.

[19] Huesmann GR, Schwarb H, Smith DR, Pohlig RT, Anderson AT, McGarry MDJ, Paulsen KD, Wszalek TM, Sutton BP, Johnson CL. Hippocampal stiffness in mesial temporal lobe epilepsy measured with MR elastography: Preliminary comparison with healthy participants. Neuroimage Clin. 2020;27:102313. doi: 10.1016/j.nicl.2020.102313. Epub 2020 Jun 16. PMID: 32585569; PMCID: PMC7322100.

[20] S. Ammar and M. Senouci. (2016). "Seizure detection with single-channel EEG using Extreme Learning Machine," 17th International Conference on Sciences and Techniques of Automatic Control and Computer Engineering (STA), Sousse, pp. 776-779, doi: 10.1109/STA.2016.7952088.